

Adaptive Learning-based Method for Nitrate Sensor Quality Assessment in On-line Scenarios*

Qingyu Yang, Kerry Maize, Ye Mi, George Chiu, Ali Shakouri, Jan Allebach
Purdue University, West Lafayette, Indiana 47906, U.S.A

Abstract

Nitrate sensors are commonly used to reflect the nitrate levels of soil conditions in agriculture. In a roll-to-roll system, for manufacturing Thin-Film nitrate sensors, varying characteristics of the ion-selective membrane on screen-printed electrodes are inevitable and affect sensor performance. It is essential to monitor the sensor performance in real-time to guarantee the quality of the products. We applied image processing techniques and off-line learning to realize the performance assessment. However, a large variation of the sensor's data with dynamic manufacturing factors will defeat the accuracy of the prediction system. In this work, our key contribution is to propose a system for predicting the sensor performance in on-line scenarios and making the neural networks efficiently adapt to the new data. We leverage residual learning and Hedge Back-Propagation to the on-line settings and make the predicting network more adaptive for input data coming sequentially. Our results show that our method achieves a highly accurate prediction performance with compact time consumption.

Introduction

Solid-contact nitrate sensors have been applied widely in agriculture. Controlling the quality of sensors is one of the essential steps of the manufacturing process. Due to different applications or manufacturing purposes, the variety of manufacturing settings makes it difficult for the off-line trained sensor assessment system to adapt to new features. Therefore, a well-developed sensor assessment system needs to predict the sensor quality accurately and adapt to the changing manufacturing settings efficiently.

The Scalable Manufacturing of Aware and Responsive Thin Films (SMART) [1] consortium is developing roll-to-roll (R2R) processing, which is an advanced scalable manufacturing method to achieve the goal of high-throughput and low-cost. The Thin-Film nitrate sensor, one of the products of SMART, is intended to be an inexpensive potentiometric nitrate sensor. These sensors are fabricated with an ion-selective membrane (ISM) [2] to realize the function of detecting nitrate levels. Fig. 1 shows the R2R system and the fabrication of the Thin-Film nitrate sensors. A physical analysis indicates that the varying roughness of the fabricated ISM is challenging to quantify and affects sensor performance. To help guide the manufacturing process, we propose an image-based on-line assessment system to monitor the nitrate

sensor quality in real-time, and to provide influential information for further manufacturing.

In our previous work [3], we designed an imaging system to capture the roughness of the sensor's active region. We verified the existing relationship between the sensor performance metrics and the 2-D images of the ISM regions in nitrate sensors. Reference [4] developed the automatic systems to predict the sensor performance based on the captured active-region images. As part of the development of the deep neural networks, many influential network structures [5, 6, 7] were adopted in image-based approaches for classification, regression, and segmentation. Due to the high-performance optimization techniques [8, 9] and the well-built datasets [10, 11] that contain extensive, quantitative data, and high-quality labels, learning-based methods can achieve promising results on the static datasets. Therefore, [4] also proposed a Convolutional Neural Networks (CNN) based approach to predict the large-scale 1-D array of performance curves to better assess the nitrate sensor's quality. Although this CNN model achieves promising results, it is an off-line learning method that trains on a static dataset and narrows to adapt to new situations, e.g., assess sensors from new manufacturing settings.

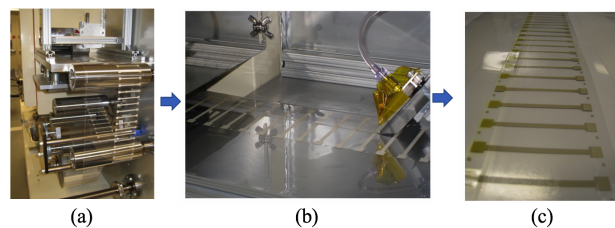


Figure 1. R2R manufacturing process of Thin-Film nitrate sensors: (a). R2R system; (b). ISM fabrication process; (c). Fabricated Thin-Film nitrate sensors on PET substrate.

Preparing a sufficient dataset for the various manufacturing settings is not always feasible in real manufacturing scenarios and limits the off-line learning method's practicality. Industry needs a more adaptive approach to train and inference the data in a timely manner. However, tuning the deep CNN model in on-line scenarios needs sufficient time for convergence. The shallower layers' parameters change slowly due to the vanishing gradient problem. To address this problem, Sahoo *et al.* [12] proposed Hedge Back-Propagation (HBP) to embed a concept of dynamic depth and help the gradients backpropagate to the shallower layers to advance the on-line learning. However, this implementation was applied for classification tasks, and the Fully-Connected (FC) network is not efficient in on-line settings. In this work, we implement the

*Research supported by the SMART Films consortium (<https://engineering.purdue.edu/SMART-consortium>).

HBP with FC network to predict sensor quality. We also apply the ResNet [6], an influential network structure that can benefit on-line setting adaptation. Finally, we use the HBP strategy in ResNet and develop the on-line learning based system to accurately predict the sensor's quality and adjust efficiently to the new manufacturing settings.

Sensor Performance Prediction in On-line Scenarios

Sensor Performance Data

To quantify the sensor performance, we need to record the temporal potentiometric voltage response in a specific nitrate solutions for around 24 hours. For real-time assessment, our system is supposed to predict the performance curve as time increases, which is a large-scale 1-D array and includes around 2k elements. However, the raw data includes inevitable noise from the manual measurement. Thus, we apply a curve fitting system to reconstruct the temporal potentiometric voltage response from the measured data to avoid the effects of the experimental error. Fig. 2 shows the curve fitting process. $V_m(t)$ represents the raw data as a function of time. We apply an average filter with a 30-length sliding window to $V_m(t)$ to eliminate the data noise. Since the measuring time intervals are different, we downsample the temporal data to 100 data points to keep a consistent length of the performance data. The last 80% of the down-sampled data points represent the potentiometric response in the saturated phase, which indicates the sensor quality. The 80-point data is labeled as $V_d(x)$ to be the curve fitting input, and the x equals 20, 21, ..., 99.

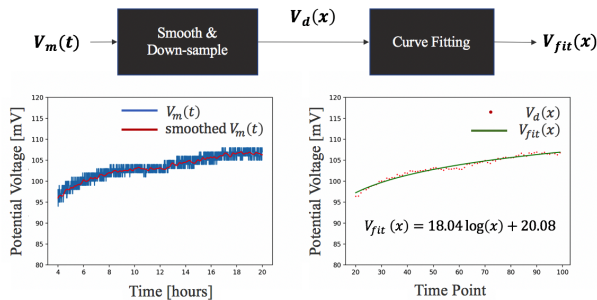


Figure 2. Curve-fitting system and an example: the left-bottom figure shows the voltage response of the original measurement and the smoothed data as a function of time in saturated phase; the right-bottom figure shows the downsampled data points and the fitted curve vs. the defined time points.

According to the ion transport equation [13], the potentiometric response exhibits logarithmic growth in the ideal case. Thus, we define the fitting model to be a logarithmic curve, as shown in Eq. 1. Here, we use the Levenberg-Marquardt algorithm [14] to optimize the parameters a and b of the fitting model. The optimized model parameters define the shape of the temporal sensor performance data of the nitrate sensor. The fitted logarithmic curve V_{fit} will be treated as the system's prediction target. We will further apply regression models to predict parameters a and b based on image features.

$$V_{fit}(x) = a \log(x) + b \quad (1)$$

Prediction System with On-line Settings

Our previous work [4] generates multiple regression models to predict the fitted curve with off-line learning. Deep learning has shown its more powerful ability to represent the distinctive features from images. The traditional machine learning system is susceptible to the hyper-parameters that makes the system hard to update in on-line settings. Thus, we expect to extend the fine-tuned CNN method to the prediction system in on-line scenarios. Off-line training optimizes the regression model by passing through the training dataset multiple times. However, in on-line scenarios, the input data come sequentially. In our task, the newly fabricated sensors come to the prediction model one by one to make a prediction and update the model in the same iteration. Fig. 3 shows the on-line prediction process during nitrate sensor manufacturing. In each iteration (t), one new sensor data will be fed to the prediction model. x_t is the incoming new sensor's active-region image, and V_t with parameters a_t and b_t represents the corresponding fitted logarithmic curve, which is the ground truth. The on-line prediction is based on the model generated at $t - 1$. After the prediction, the loss between the current prediction and the ground truth will be applied to train the model for adapting the characteristics to the new input.

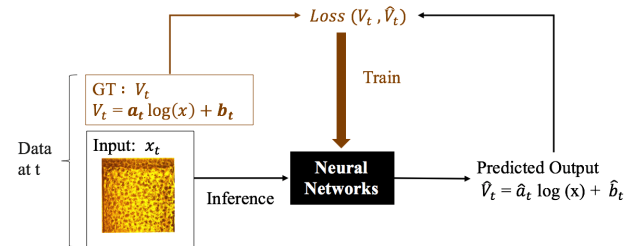


Figure 3. On-line system for predicting the nitrate sensor performance based on 2D images at iteration t .

Proposed Method

In this implementation, we first apply the original Hedge Back-Propagation (HBP) network [12] for the on-line regression. We then investigate the backbone network structure and choose the ResNet, a network based on residual learning that can efficiently adapt to on-line scenarios, for on-line regression learning. We finally design an on-line learning network that is based on ResNet and embed the optimizing strategy of HBP.

Fully Connected Network with Hedge Back-propagation

HBP was proposed by [12]. It provides shortcuts for gradient backpropagation, and dynamically selects the model's depth to improve the on-line classification performance. In this work, we follow this concept and implement with a 4-layer FC network, as shown in Fig. 4. The entire backbone network follows the conventional FC network design that all layers are in sequence and fully connect to the next layer. The non-linear activation function, ReLU, is placed after each FC layer to learn the high-level feature representations. The input image will be first resized to $224 \times 224 \times 3$ and then flattened as a 1-D vector and fed to our network. All FC layers in our network produce 1,024-dimension feature vectors. Unlike classical FC networks, the 4 FC layers'

outputs can be treated as feature maps to directly estimate the results. To meet the goal of regression task, each of the 4 regression layers contains two neurons to predict the parameters a and b in Eq. 1.

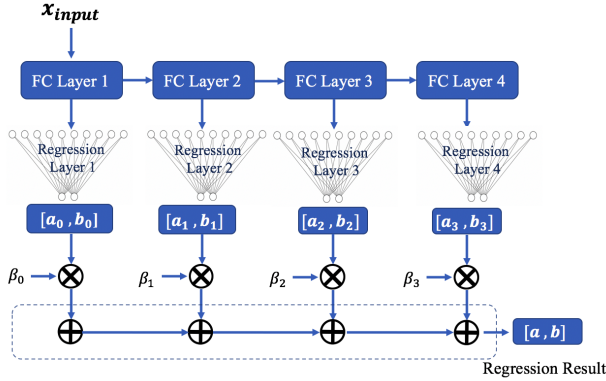


Figure 4. The input x_{input} is a flattened image that is fed to a 4-layer FC network. All four FC layers output a 1,024 dimension feature vector and transmit to regression layers for regressions. The final regression result is a weighted sum of each layer's regression. The weights β_i are trainable parameters.

The final output is a weighted sum of the 4 layers' regression results. β_i is a trainable weight of the i -th layer that optimized by Eq. 2, where t represents the updating iteration and γ is a discount rate with the value of 0.99. The updated β_i is determined by the i -th layer's loss, \mathcal{L}_i . A larger \mathcal{L}_i will generate a smaller β_i . After each update, we normalize the weights so that $\sum \beta_i = 1$. Therefore, based on the current loss of each layer, the system will assign the β_i to optimize the overall performance. For example, suppose the shallower layer's regression performance is better than that of the deeper layers. In that case, the β corresponding to the shallower layer will be larger due to its lower loss value.

The loss of the i -th layer is calculated based on Eqs. 3 and 4. As shown in Eq. 3, each layer has predicted $(a_{i,p}, b_{i,p})$ for Eq. 4, which is compared with the reference ground-truth (a_{gt}, b_{gt}) for loss calculation. Eq. 4 presents the logarithmic curve based on our physics-model assumption and x represents 80 sampled time points. The Root Mean Square Error (RMSE), between the predicted logarithmic curve and ground-truth curve, will be used for loss calculation. It is worth mentioning that the shallower layers commonly converges faster than the deeper layers. Therefore, based on our β_i updating strategy, the β_i of the shallower layers would be much larger than that of the deeper layer at the beginning and cause the network to keep focusing on the shallower layers' performance. To alleviate this, we set a minimum boundary $\frac{s}{L}$ to β_i so that β_i will not be too small to ignore the corresponding layer during the training process. The parameter L is the total number of FC layers, which is 4 in our implementation. Following the optimal setting in [12], we set s to be 0.2.

$$\beta_i^{(t+1)} = \beta_i^{(t)} \gamma^{\mathcal{L}_i} \quad (2)$$

$$\mathcal{L}_i((a_{i,p}, b_{i,p}), (a_{gt}, b_{gt})) = RMSE(F(a_{i,p}, b_{i,p}), F(a_{gt}, b_{gt})) \quad (3)$$

$$F(a, b) = a \log(x) + b \quad \text{for } x = 20, 21, \dots, 99 \quad (4)$$

ResNet for On-line Learning

The convolutional kernel and the pooling layers in a CNN can learn both the image's local features and global features. Due to their efficiency and strong learning ability, many developed CNN structures have also been implemented for the on-line tasks. Although the deeper CNN models commonly outperform shallower models, they suffer from many convergence issues, e.g., gradient vanishing and training time consumption. For example, based on the Chain Rule [15], the loss backpropagates to the first layer from L -th layer by multiplying L partial derivatives. If all partial derivatives are smaller than 1, the final gradients returning to the shallower layers will become too small to update the weights. To overcome this issue, deep neural networks trained on static datasets usually consume meaningful time for convergence.

On-line learning model, trained on the data in sequence, cannot provide sufficient time for a deep network, such as VGG [5], to converge. However, He et al. [6] proposed residual learning, which inserts a skip connection between each block of convolutional layers. As shown in Fig 5, those connections provide the shortcuts for gradient propagation to reduce the convergence time of the shallower layers. Therefore, ResNet is a potential backbone network for efficient on-line learning. In our work, the ResNet

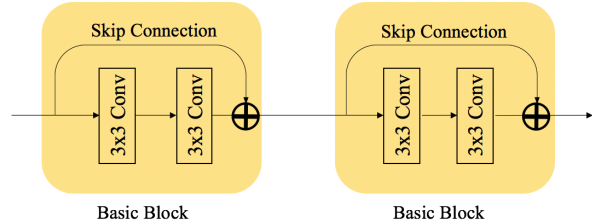


Figure 5. An example of two basic block in sequence. During the back-propagation, the gradient in the output layer can directly pass to the shallow layers.

was first trained on the off-line dataset and then applied under the on-line settings. In other words, the ResNet will take a single new sensor image in the sequence and tune itself with this input for several cycles. We choose a small learning rate during the on-line training to avoid overshooting. Also, we control the number of cycles to get optimal performance.

ResNet with Hedge Back-Propagation

Although the residual learning helps the ResNet transmit the gradient from the deeper layer to the shallower layer, the fixed depth still limits its on-line learning performance. In this work, we implement the HBP's dynamic depth concept and combine it with the ResNet-34 for on-line sensor image assessment. As shown in Fig. 6, the conventional ResNet can be split into four stages; and each stage generates a feature map with different channels. As shown in Table 1, the ResNet-34 in our implementation has 256-D, 512-D, 1024-D, and 2048-D feature maps. A stride convolutional layer between two stages downsamples the feature map and increases the receptive area. Therefore, the ResNet can learn more global features from the image.

To apply those intermediate layers' feature maps for regression, we insert a global average pooling layer to summarize the feature maps at the end of each stage. Regression layers with two

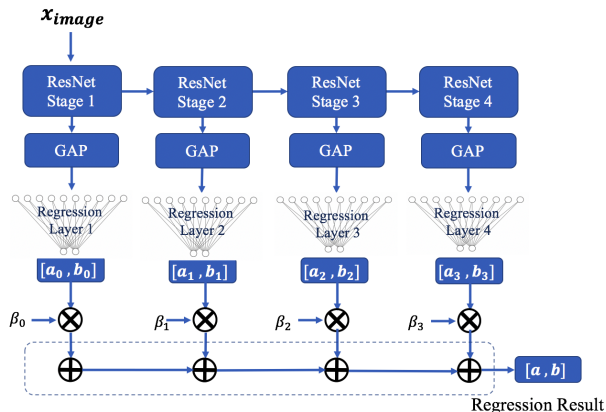


Figure 6. An image will first be resized to $224 \times 224 \times 3$ and fed to our network for regression. Each stage outputs different dimension feature maps. We apply Global Average Pooling (GAP) to transfer the feature maps to feature vectors and do regression task. The final regression result is a weighted sum of all 4 regression results.

Table 1: Feature map dimension of 4 stages of ResNet-34.

	Dimension
Stage 1	$56 \times 56 \times 256$
Stage 2	$28 \times 28 \times 512$
Stage 3	$14 \times 14 \times 1024$
Stage 4	$7 \times 7 \times 2048$

neurons will fully connect to each feature vector for assessment parameter prediction. Our final regression result is a weighted sum of 4 regression outputs of all the stages. Following Eq. 2, the weight parameter β_i is also a trainable parameter. All the β_i will be normalized after each updating and have a minimum boundary $\frac{\epsilon}{L}$. Instead of SGD [8], which used in the original implementation [12], we choose Adam [9] to update all other parameters in the model.

Experiments

We generate our Thin-Film nitrate sensor dataset with varying manufacturing factors to evaluate the proposed on-line learning methods. In the on-line prediction system, the recent data will be used one by one to train and inference the model. In addition, the initial weights of the models are fine-tuned from an off-line dataset. The off-line dataset simulates the data that we have seen before the manufacturing.

Dataset Preparation

Our nitrate sensor dataset includes the active-region images of the nitrate sensors and the measured potentiometric response of each sensor. We follow the imaging system in our previous work [3] to capture the roughness of the membrane and apply edge detection to crop the active region and eliminate the effect of the background. The detecting system is generated in real-time and can embed into an on-line camera system. In addition, the corresponding sensor performance is measured in a 0.001 M nitrate solution for around 24 hours. The performance metric is the

difference between the potential voltages of the target membrane and a reference sensor.

Fig. 7 shows the samples of our Thin-Film nitrate sensor dataset. Since the sensors are manufactured on different dates with varying manufacturing factors, we group the sensors' data by the manufacturing runs. We separate our dataset into an off-line dataset and an on-line dataset to mimic the manufacturing process. The off-line dataset includes three earlier groups with a total of 97 sensors; and the on-line dataset includes two alternative groups with a total of 45 sensors. Fig. 7(a) shows examples from each group for the captured active-region images as judged by visual perception. Fig. 7(b) shows that their potentiometric response also grows according to different behaviors. The off-line dataset will be used to fine-tune the neural networks for the initialization of on-line learning networks. Subsequently, the on-line dataset will be fed to prediction systems under the on-line settings.

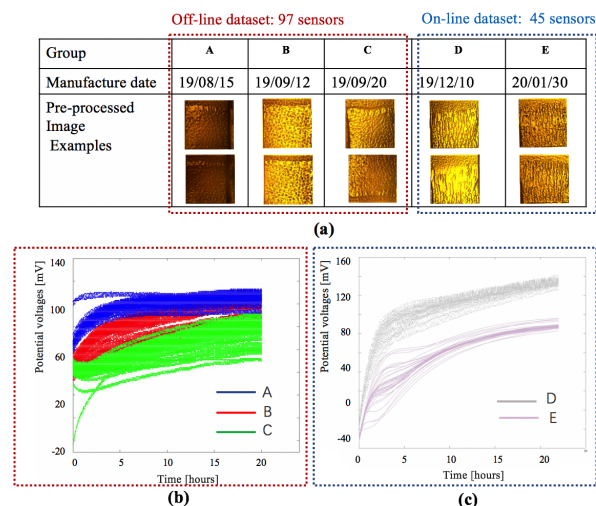


Figure 7. Nitrate sensor dataset from different manufacturing runs (red box includes off-line dataset; blue box includes on-line dataset): (a). Example active-region images in different groups; (b). Potentiometric voltage response measured in 0.001 M nitrate solution for sensors in the off-line dataset; (c). Potentiometric voltage response measured in 0.001 M nitrate solution for sensors in the on-line dataset.

As we mentioned before, we apply the curve fitting method to all the measured performance data. The fitted logarithm curve $V_{fit}(x)$ as a function of increasing time points is the ground truth or the prediction target. The average RMSE of the fitted curve $V_{fit}(x)$ and the down-sampled curve $V_d(x)$ across the entire dataset is 1.39%. We conclude that the fitted curves can depict the original measurements.

Baseline Experiments

We first apply the proposed architectures: HBP, ResNet, and ResNet with HBP, to predict the sensor performance curve with off-line settings. We use the off-line dataset in training and the on-line dataset in the inference part. In the training process, we randomly select 90 sensors for training and the remaining 7 sensors for validation to prevent overfitting. In the implementation of the ResNet-34 model, we use pre-trained weights, which are trained on ImageNet, as initial values to help provide faster convergence in training. After 2k epochs with the three models, both train-

Table 2: Loss in training, validation, and inference in three methods with off-line settings.

Method	Train Loss [mV]	Validation Loss [mV]	Test Loss [mV]
ResNet + BP	1.63	7.98	21.69
FC + HBP	3.34	8.76	30.90
ResNet + HBP	5.14	6.93	23.95

ing loss and validation loss converge. Table 2 shows the results of training, validation, and inference loss with the three methods. The varying data distributions among the different manufacturing runs limit the model’s generalization performance. Thus, the testing loss of on-line dataset is much higher than the training/validation loss.

Evaluation Metrics of On-line Learning

We apply the three methods as described in the section on the proposed methods. We assume that the prediction models have seen the off-line dataset, which is from earlier manufacturing runs. Thus, the initial weights of the three methods are generated by fine-tuning the networks on the off-line dataset to efficiently adapt to the new sensor data. In the on-line prediction, the on-line dataset with 45 sensors comes to the prediction model one by one. The current prediction’s loss will backpropagate the model and update the neural network multiple times for higher accuracy in each iteration. We need to optimize the number of cycles, i.e. the updating times within each iteration to achieve more accurate and preventing overfitting. The evaluation system for on-line learning is placed at the start of each iteration. The RMSE is applied to quantify the prediction error. Eq. 5 shows the calculation of the RMSE at the t -th iteration. The total time cost is also an essential metric to evaluate the efficiency of our prediction model.

$$RMSE_t = \sqrt{\frac{1}{N} \sum_{x=20}^{99} (V_t(x) - \hat{V}_t(x))^2} \quad (5)$$

$$RMSE_{AVG} = \frac{\sum_{t=1}^T RMSE_t}{T} \text{ for } T = 45 \quad (6)$$

Results and Discussion

In the on-line learning experiment, the evaluation and training processes occur simultaneously. To fairly compare the three methods’ adaptive abilities, we apply the optimal numbers of cycles to achieve the best performance for each model. Fig. 8 shows the RMSE of the prediction with new data coming in each iteration. The RMSE suddenly increases when the sensor from an unseen group coming into the prediction model. Then, the prediction errors descend within one iteration. Table 3 compares the average RMSE, which is shown in Eq. 6, and the time cost for each coming new sensor in the on-line training process. According to our results, the FC layers with HBP obtain the smallest prediction error with the on-line settings. But the HBP optimization method is more suitable under on-line scenarios, since the training process of the FC layers costs much more time than the ResNet architectures due to the large number of parameters in the FC layers. Our proposed method of leveraging the ResNet architecture with HBP optimization also achieves higher accuracy than

Table 3: Results of RMSE and computation time in on-line prediction among three methods.

Method	# of cycles per sensor	$RMSE_{AVG}$ [mV]	Time cost [seconds per sensor]
ResNet + BP	30	11.76	1.20
FC + HBP	35	8.18	77.01
ResNet + HBP	20	10.06	4.91

the method of ResNet with conventional backpropagation. On the other hand, it also largely reduces the training time compared to the model of stacking FC layers. The proposed approach leverages residual learning’s efficient architecture to keep updating the prediction model in real-time. Also, it applies the novel optimization method of HBP to achieve higher accuracy during the on-line task.

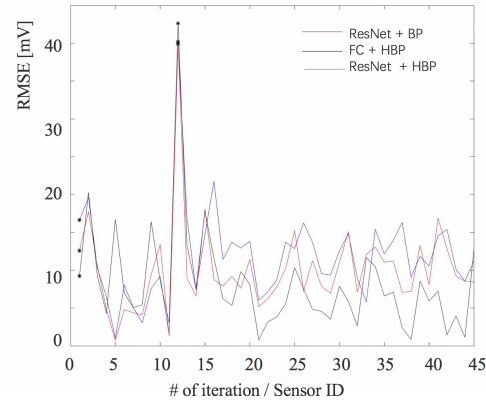


Figure 8. Comparison of adaptive abilities for three methods: RMSE between prediction and ground truth for 45 nitrate sensors in on-line settings with three developed methods; * represents data with unseen manufacturing runs coming to the prediction model.

Conclusion

In this paper, we implement three different network structures for the Thin-Film sensor’s assessment task. The original FC + HBP achieves the best assessment performance. However, due to the network structure, the FC + HBP needs expensive time consumption for tuning. Both ResNet-34 with conventional backpropagation (ResNet + BP) and ResNet with HBP (ResNet + HBP) can assess the sensor’s performance in real-time. Due to the advantages of HBP, the ResNet + HBP can provide better assessment performance than ResNet + BP. Therefore, the ResNet + HBP not only uses the HBP for better on-line assessment performance, but also efficiently adapts to new manufacturing settings by benefiting from the ResNet’s structure.

Besides the prediction method based on surface roughness images, we are also investigating more on-line measured data, such as coating thickness, and electrical properties etc., to help guide the manufacturing. In the next step, we can also fuse more additional real-time inputs of fabricated sensors to captured images and develop a more accurate prediction model.

References

- [1] "SMART Films Consortium," Brick Nanotechnology Center, Purdue University, West Lafayette, IN. [Online]. Available: <https://engineering.purdue.edu/SMART-consortium>
- [2] J. Hu, A. Stein, and P. Bühlmann, "Rational design of all-solid-state ion-selective electrodes and reference electrodes," *TrAC Trends in Analytical Chemistry*, vol. 76, pp. 102–114, 2016.
- [3] Q. Yang, Y. Yan, K. Maize, X. Jin, H. Jiang, M. A. Alam, B. Ziaie, G. Chiu, A. Shakouri, and J. P. Allebach, "Image based quality assurance of fabricated nitrate sensor," *NIP & Digital Fabrication Conference*, 2019.
- [4] Q. Yang, K. Maize, X. Jin, H. Jiang, M. A. Alam, R. Rahimi, G. Chiu, A. Shakouri, and J. P. Allebach, "Predicting response of printed potentiometric nitrate sensors using image based machine learning," *NIP & Digital Fabrication Conference*, 2020.
- [5] K. Simonyan and A. Zisserman, "Very deep convolutional networks for large-scale image recognition," *arXiv preprint arXiv:1409.1556*, 2014.
- [6] K. He, X. Zhang, S. Ren, and J. Sun, "Deep residual learning for image recognition," *Proceedings of the IEEE Conference on Computer Vision and Pattern Recognition*, pp. 770–778, 2016.
- [7] G. Huang, Z. Liu, L. Van Der Maaten, and K. Q. Weinberger, "Densely connected convolutional networks," *Proceedings of the IEEE Conference on Computer Vision and Pattern Recognition*, pp. 4700–4708, 2017.
- [8] H. Robbins, "A stochastic approximation method," *Annals of Mathematical Statistics*, vol. 22, pp. 400–407, 2007.
- [9] D. P. Kingma and J. Ba, "Adam: A method for stochastic optimization," *arXiv preprint arXiv:1412.6980*, 2014.
- [10] J. Deng, W. Dong, R. Socher, L.-J. Li, K. Li, and L. Fei-Fei, "ImageNet: A Large-Scale Hierarchical Image Database," *Proceedings of the IEEE Conference on Computer Vision and Pattern Recognition*, 2009.
- [11] A. Krizhevsky, G. Hinton *et al.*, "Learning multiple layers of features from tiny images," 2009.
- [12] D. Sahoo, Q. Pham, J. Lu, and S. C. Hoi, "Online deep learning: Learning deep neural networks on the fly," *arXiv preprint arXiv:1711.03705*, 2017.
- [13] J. T. Stock and M. V. Orna, *Electrochemistry, Past and Present*. Washington, DC: American Chemical Society, 1989, vol. 390.
- [14] J. J. Moré, "The Levenberg-Marquardt algorithm: implementation and theory," in *Numerical analysis*. Berlin, Heidelberg: Springer, 1978, pp. 105–116.
- [15] A. G. Baydin, B. A. Pearlmutter, A. A. Radul, and J. M. Siskind, "Automatic differentiation in machine learning: a survey," *The Journal of Machine Learning Research*, vol. 18, no. 1, pp. 5595–5637, 2017.

Author Biography

Qingyu Yang received her B.S. (2017) and M.S. (2019) in Electrical Engineering from Purdue University and currently is Ph.D. candidate in Purdue ECE. Her research focuses on image quality analysis, computer vision, object detection, and deep learning applications.

Kerry Maize received his B.S. in Electrical Engineering and Computer Science from UC Berkeley in 2002. He came to UCSC in 2005 to pursue graduate study in the areas of quantum electronics and nanoscience. His current work is focused on optical coherence tomography, and thermal device characterization. Prior to engineering Kerry worked in journalism.

Mi Ye received his Ph.D. in Nuclear Engineering from Purdue University in 1998. He received both his M.S. and B.S. from Tsinghua University in China, majoring in Nuclear Physics and Nuclear Instrumentation respectively. In recent years, he has been focusing on RD of industrial processing tomography. Currently, he is working on inline metrology of $r2r$ systems.

George T.C. Chiu is a Professor of Mechanical Engineering with courtesy appointments in Electrical and Computer Engineering and Psychological Sciences at Purdue University. He received the B.S. degree from National Taiwan University and the M.S. and Ph.D. degrees from University of California at Berkeley. His research interests are mechatronics and control with applications to digital printing and imaging systems, digital fabrications and functional printing. He is a Fellow of ASME and IS&T.

Ali Shakouri is a professor of electrical and computer engineering and director of Birck Nanotechnology Center at Purdue University. He received his PhD from Caltech. His current research is on nanoscale heat transport and electrothermal energy conversion. He has developed lock-in imaging for temperature measurement and for real-time monitoring of functional film manufacturing. He is also leading a team to manufacture low-cost smart internet of thing (IoT) devices and sensor network for applications in advanced manufacturing and agriculture.

Jan P. Allebach is Hewlett-Packard Distinguished Professor of Electrical and Computer Engineering at Purdue University. Allebach was named Electronic Imaging Scientist of the Year by IS&T and SPIE, and was named Honorary Member of IS&T, the highest award that IS&T bestows. He has received the IEEE Daniel E. Noble Award, the IS&T/OSA Edwin Land Medal, the IS&T Johann Gutenberg Prize, is a Fellow of the National Academy of Inventors, and is a member of the National Academy of Engineering.

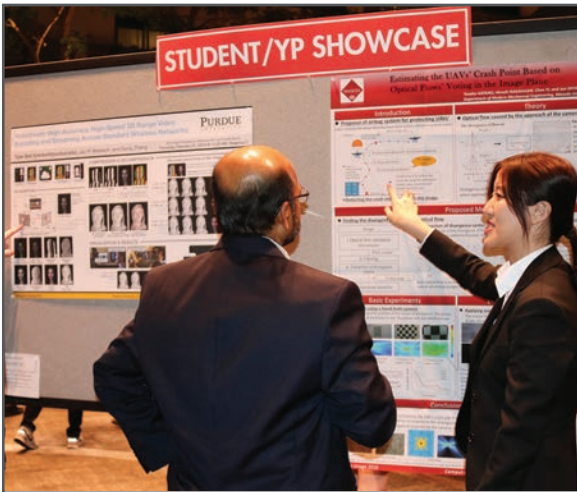
JOIN US AT THE NEXT EI!

IS&T International Symposium on

Electronic Imaging

SCIENCE AND TECHNOLOGY

Imaging across applications . . . Where industry and academia meet!



- **SHORT COURSES • EXHIBITS • DEMONSTRATION SESSION • PLENARY TALKS •**
- **INTERACTIVE PAPER SESSION • SPECIAL EVENTS • TECHNICAL SESSIONS •**

www.electronicimaging.org

